A statistical solution to the chaotic, non-hierarchical three-body problem

https://doi.org/10.1038/s41586-019-1833-8

Received: 4 February 2019

Accepted: 28 September 2019

Published online: 18 December 2019

Nicholas C. Stone[1,2,3]* & Nathan W. C. Leigh[4,5]

The three-body problem is arguably the oldest open question in astrophysics and has resisted a general analytic solution for centuries. Various implementations of perturbation theory provide solutions in portions of parameter space, but only where hierarchies of masses or separations exist. Numerical integrations[1] show that bound, non-hierarchical triple systems of Newtonian point particles will almost[2] always disintegrate into a single escaping star and a stable bound binary[3,4], but the chaotic nature of the three-body problem[5] prevents the derivation of tractable[6] analytic formulae that deterministically map initial conditions to final outcomes. Chaos, however, also motivates the assumption of ergodicity[7–9], implying that the distribution of outcomes is uniform across the accessible phase volume. Here we report a statistical solution to the non-hierarchical three-body problem that is derived using the ergodic hypothesis and that provides closed-form distributions of outcomes (for example, binary orbital elements) when given the conserved integrals of motion. We compare our outcome distributions to large ensembles of numerical three-body integrations and find good agreement, so long as we restrict ourselves to 'resonant' encounters[10] (the roughly 50 per cent of scatterings that undergo chaotic evolution). In analysing our scattering experiments, we identify 'scrambles' (periods of time in which no pairwise binaries exist) as the key dynamical state that ergodicizes a non-hierarchical triple system. The generally super-thermal distributions of survivor binary eccentricity that we predict have notable applications to many astrophysical scenarios. For example, non-hierarchical triple systems produced dynamically in globular clusters are a primary formation channel for black-hole mergers[11–13], but the rates and properties[14,15] of the resulting gravitational waves depend on the distribution of post-disintegration eccentricities.

The three-body problem is a prototypical example of deterministic chaos[5], in that tiny perturbations in the initial conditions (or errors in numerical integration) lead to exponentially divergent outcomes[16]. Chaotic systems often 'forget' their initial conditions (aside from integrals of motion), although this is by no means guaranteed—indeed, the topology of the chaotic three-body problem does contain islands of regularity[17,18]. Nonetheless, to a first approximation, it is reasonable to estimate the probability of different outcomes by invoking the ergodic hypothesis[7,19] and to assume that non-hierarchical triples will uniformly explore the phase-space volume accessible to them[8]. In this way, we may turn the chaotic nature of the three-body problem[5,16]—which has so far frustrated general, deterministic, analytic mappings from one set of initial conditions to one set of outcomes—into a tool that simplifies the mapping from distributions of initial conditions to distributions of outcomes.

We consider the generic outcome of the non-hierarchical Newtonian three-body problem: a single escaper star with mass m_s departs from a surviving binary with mass $m_B = m_a + m_b$, where m_a and m_b are the component masses. In Fig. 1 we illustrate this scenario, using both a direct numerical integration of the equations of motion and a schematic diagram of a metastable triple at the moment of breakup. At the time of disintegration, the binary components are separated by a distance $\mathbf{r}$ and have relative momentum $\mathbf{p}$, and the escaper is separated from the binary centre of mass by $\mathbf{r}_s$ and is moving with relative momentum $\mathbf{p}_s$. The total energy and angular momentum of the system, inherited from the initial conditions and preserved through a period of chaotic three-body interactions, are E_0 and $\mathbf{L}_0$, respectively. For convenience, we define the additional masses $M = m_s + m_B$, $m = m_B m_s/M$ and $\mathcal{M} = m_a m_b/m_B$. The total accessible phase volume for this system is that of an eight-dimensional hypersurface[8]:

$$\sigma = \int \ldots \int \delta(E_B + E_s - E_0)\delta(\mathbf{L}_B + \mathbf{L}_s - \mathbf{L}_0)\mathrm{d}\mathbf{r}\mathrm{d}\mathbf{p}\mathrm{d}\mathbf{r}_s\mathrm{d}\mathbf{p}_s \quad (1)$$

shaped by the requirements of energy and angular-momentum conservation for both the elliptic orbit of the surviving binary (E_B, $\mathbf{L}_B$) and the hyperbolic orbit between the binary and the escaper (E_s, $\mathbf{L}_s$). In

[1]Columbia Astrophysics Laboratory, Columbia University, New York, NY, USA. [2]Racah Institute of Physics, The Hebrew University, Jerusalem, Israel. [3]Department of Astronomy, University of Maryland, College Park, MD, USA. [4]Departamento de Astronomia, Facultad de Ciencias Fisicas y Matemàticas, Universidad de Concepciòn, Concepciòn, Chile. [5]Department of Astrophysics, American Museum of Natural History, New York, NY, USA. *e-mail: nicholas.stone@mail.huji.ac.il

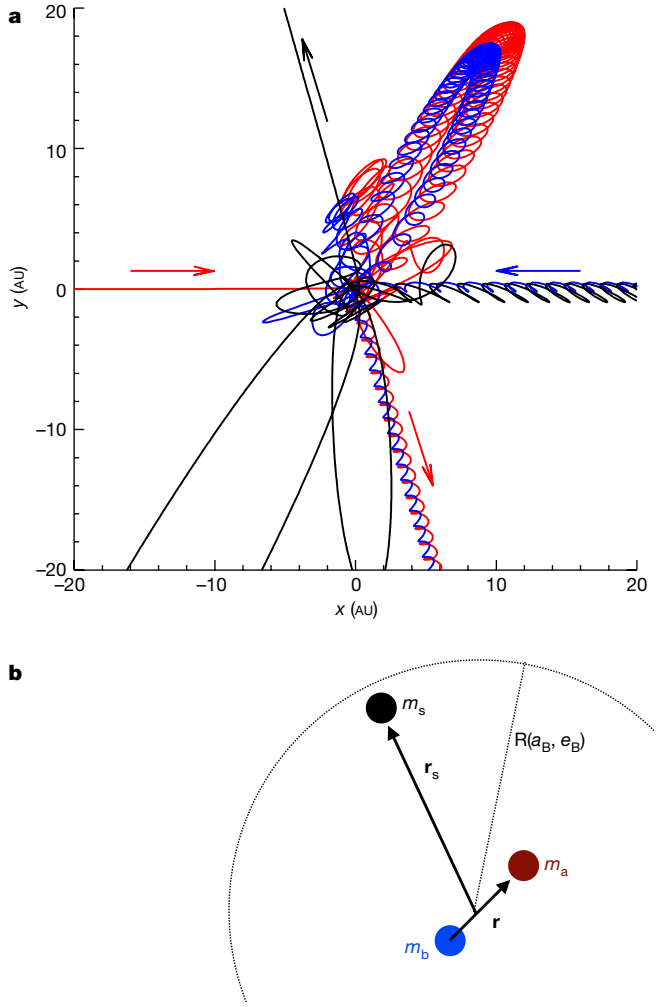

Fig. 1 | Non-hierarchical three-body scatterings. a, Two-dimensional projection of an equal-mass resonant scattering encounter, where an interloper star (red) encounters a binary (blue and black). The resonant interaction unfolds over several dynamical times before the system disintegrates in a partner swap. **b**, Schematic illustration of the metastable triple at the moment of disintegration.

equation (1), δ represents the Dirac delta function. Given a microcanonical ensemble of non-hierarchical triples with different initial conditions but identical integrals of motion and mass combinations, the outcome states (after breakup) will—assuming ergodicity—uniformly populate the phase volume that is accessible at the moment of disintegration. This ensemble is microcanonical in the sense that each three-body system is isolated from external sources of heat, but is unusual in its low particle number[7].

We evaluate this integral at the moment of disintegration, which we idealize as occurring anywhere inside a 'strong interaction region' of radius $R(E_B, L_B, C_B)$, where $C_B = \hat{\mathbf{L}}_B \cdot \hat{\mathbf{L}}_0$. Canonical transformations to elliptic/hyperbolic Delaunay elements facilitate the integration (see Supplementary Information) and yield a phase volume of

$$\sigma = \frac{2\pi^4 G^2 M^{5/2} m_B}{(m_a m_b m_s)^{3/2}} \iiint \frac{L_B \mathrm{d}E_B \mathrm{d}L_B \mathrm{d}C_B}{L_s(-E_B)^{3/2}(E_0 - E_B)^{3/2}} \times \left[\sqrt{\frac{2M(E_0 - E_B)}{G^2 m_s^3 m_B^3}} \sqrt{2m(E_0 - E_B)R^2 + 2GMm^2 R - L_s^2} - \mathrm{acosh}\left(\frac{1 + [2(E_0 - E_B)R/(Gm_s m_B)]}{\sqrt{1 + [2M(E_0 - E_B)L_s^2/(G^2 m_s^3 m_B^3)]}} \right) \right] \quad (2)$$

where G is Newton's gravitational constant. For brevity, we have re-inserted the angular momentum of the escaping star, $L_s^2(L_B, C_B) \equiv L_B^2(1 - C_B^2) + (L_B C_B - L_0)^2$. σ is a phase volume and the integrand of equation (2) is a trivariate outcome distribution representing the differential probability of finding a disintegrating metastable triple in a volume $\mathrm{d}E_B \mathrm{d}L_B \mathrm{d}C_B$: the microcanonical ensemble for survivor binaries produced in the non-hierarchical three-body problem (other—angular—binary orbital elements are distributed uniformly). Therefore, specification of the total energy E_0 and the total angular momentum $\mathbf{L}_0$ suffices to describe the distribution of outcomes in non-hierarchical triple systems, even if this information alone cannot deterministically specify how one individual outcome follows from one set of initial conditions. Conservation of E_0 and $\mathbf{L}_0$ means that the trivariate outcome distribution in equation (2) can be mapped one to one to the distribution of escaper properties. Equation (2) makes fewer simplifying assumptions than did past ergodic analyses of the general three-body problem[8,9,20,21], and its outcome distributions are qualitatively different.

We marginalize over L_B and C_B to compute the distribution of outcome energies, $\mathrm{d}\sigma/\mathrm{d}E_B$. In this and all remaining calculations, we assume that the strong interaction region is a dimensionless multiple of the time-averaged binary size, that is, $R = \alpha a_B(1 + e_B)$, where $\alpha \approx 1$ is a dimensionless constant (see Extended Data Figs. 1–3 and Supplementary Information for more details). In an $L_0 = 0$ ensemble, this is $\mathrm{d}\sigma/\mathrm{d}E_B \propto |E_B|^{-7/2}$, extending to $|E_B| \to \infty$. Conversely, when L_0 is large, the ergodic energy distribution is slightly steeper, changing roughly as $\mathrm{d}\sigma/\mathrm{d}E_B \propto |E_B|^{-4}$, but only up to a maximum energy of $|E_{max}| \propto L_0^{-2}$; larger outcome energies are prohibited by angular-momentum conservation. The energy distribution that we calculate differs from past estimates determined assuming detailed balance[10], demonstrating that a population of binaries engaging in resonant three-body interactions with a thermal bath of single stars cannot achieve detailed balance, so long as their outcomes are ergodically distributed.

We likewise integrate to find the marginal outcome distributions in angular momentum (which we represent in terms of binary eccentricity e_B, as $\mathrm{d}\sigma/\mathrm{d}e_B$) and inclination ($\mathrm{d}\sigma/\mathrm{d}C_B$). In contrast to the usual (although not universal[22]) expectation of a thermal eccentricity distribution, $\mathrm{d}\sigma/\mathrm{d}e_B = 2e_B$, we find a mildly super-thermal eccentricity distribution for large L_0: $\mathrm{d}\sigma/\mathrm{d}e_B = \frac{6}{5}e_B(1 + e_B)$. This radial orbit bias is a geometric effect arising from the larger average interaction cross-section of a highly eccentric binary, the apocentre of which is twice as large as that of a circular binary of equal energy. In the low-L_0 limit, the ergodic distribution of survivor eccentricities is highly super-thermal, with $\mathrm{d}\sigma/\mathrm{d}e_B \propto e_B(1 + e_B)/\sqrt{1 - e_B^2}$ when $L_0 = 0$. There is a strong bias towards producing nearly radial binaries as a consequence of angular-momentum starvation: whereas a low-L_0 ensemble of non-hierarchical triples may produce a quasi-circular survivor binary, doing so requires substantial fine-tuning of the angle and velocity of the escaper, and is therefore disfavoured. Similar phase volume considerations explain the strong bias towards prograde ($0 < C_B \leq 1$) orbits predicted by equation (2) when marginalized into $\mathrm{d}\sigma/\mathrm{d}C_B$. More detailed explorations of the ergodic $\mathrm{d}\sigma/\mathrm{d}E_B$, $\mathrm{d}\sigma/\mathrm{d}e_B$ and $\mathrm{d}\sigma/\mathrm{d}C_B$ distributions are shown in Extended Data Figs. 1, 2, 3, respectively, as well as in Supplementary Information.

Our outcome distribution, $\mathrm{d}\sigma/(\mathrm{d}E_B \mathrm{d}L_B \mathrm{d}C_B)$, was derived with several assumptions, most notably: (i) the ergodic hypothesis, (ii) instantaneous disintegration and (iii) a specific parameterization of the 'strong interaction region' defining the limits of integration. It should therefore be tested against ensembles of numerical scattering experiments. We have explored the ergodicity of non-hierarchical triples in the equal-mass limit by using the FEWBODY numerical scattering code to run three ensembles of different binary–single scattering experiments (see Extended Data Table 1). Each ensemble has roughly $N \approx 10^5$ runs with constant E_0 and L_0, but otherwise random initial conditions (we initialize our binary–single scatterings with zero impact parameter, so we can

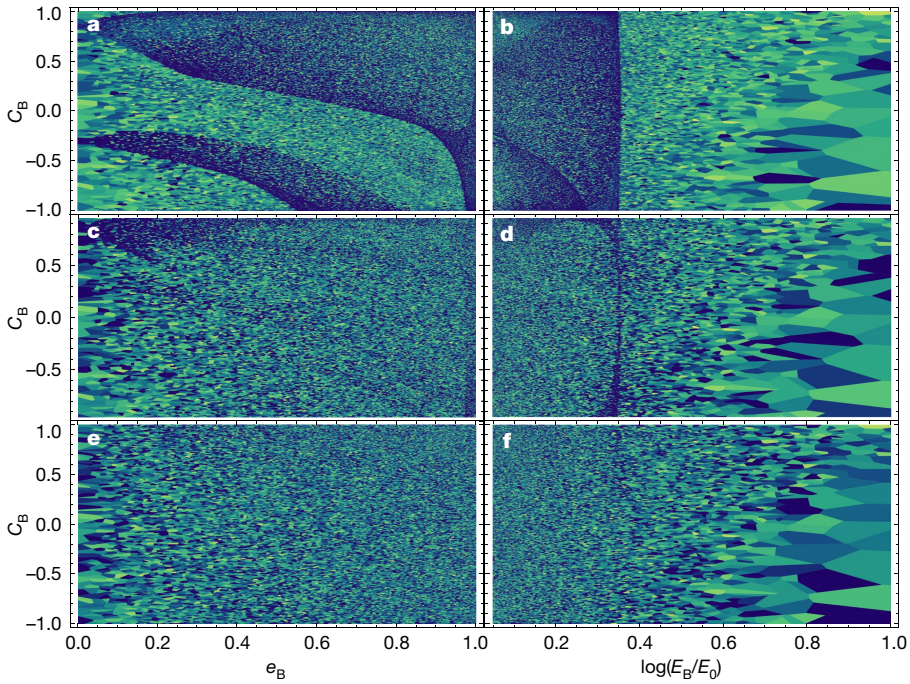

Fig. 2 | Topological maps of three-body scattering outcomes for run A. a–f, The total number of scrambles is colour-coded (smallest values of N_{scram} as dark blue, larger N_{scram} in green and yellow) with logarithmic scaling, as a function of survivor binary eccentricity e_B (**a**, **c**, **e**), energy E_B (**b**, **d**, **f**) and cosine inclination C_B. Shown are the cases $N_{scram} \geq 0$ (**a**, **b**), $N_{scram} \geq 1$ (**c**, **d**) and $N_{scram} \geq 2$ (**e**, **f**). Clouds of regularity obscure the underlying chaotic sea in **a**, **b**, but have dissipated in **e**, **f**, indicating that scrambles are the key dynamical mechanism responsible for 'ergodicizing' the comparable-mass three-body problem.

parametrize L_0 in terms of the initial binary eccentricity e_0). However, many of our scattering experiments do not form resonant three-body systems, but instead resolve abruptly in a prompt exchange, where it is unlikely that the ergodic hypothesis can be applied. Metastable three-body systems generally exhibit intermittent chaos[23]. Long periods of quasi-regular evolution occur during the non-terminal ejection of a single star, but these are then interrupted by brief periods of intensely chaotic evolution when that star returns to the pericentre[4,10]. We hypothesize that the degree of ergodicity in a subset of scattering experiments can be inferred from the number of scrambles, N_{scram}.

We illustrate the development of ergodicity in Fig. 2, which shows topological maps in outcome space. Whereas the full scattering ensemble

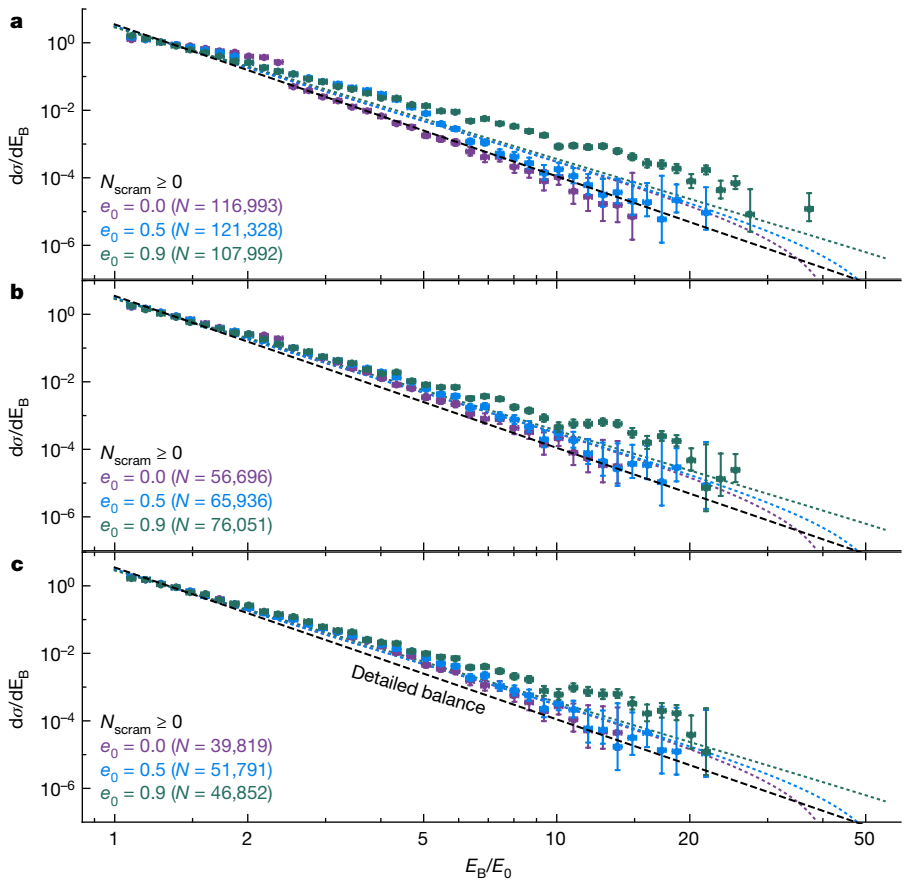

Fig. 3 | Marginal distribution of binary energy, $d\sigma/dE_B$, as a function of dimensionless energy, E_B/E_0. The dotted lines are ergodic outcome distributions for ensembles with high (purple), medium (blue) and low (green) angular momentum. The data points are binned outcomes from numerical binary–single scattering ensembles ($N \approx 10^5$). Horizontal error bars show bin sizes and vertical error bars indicate 95% Poissonian confidence intervals. **a**, Full set of results from our numerical scattering experiments. **b**, Subset of results for $N_{scram} \geq 1$. **c**, Subset of results for $N_{scram} \geq 2$. Detailed balance (black dashed line) is never achieved.

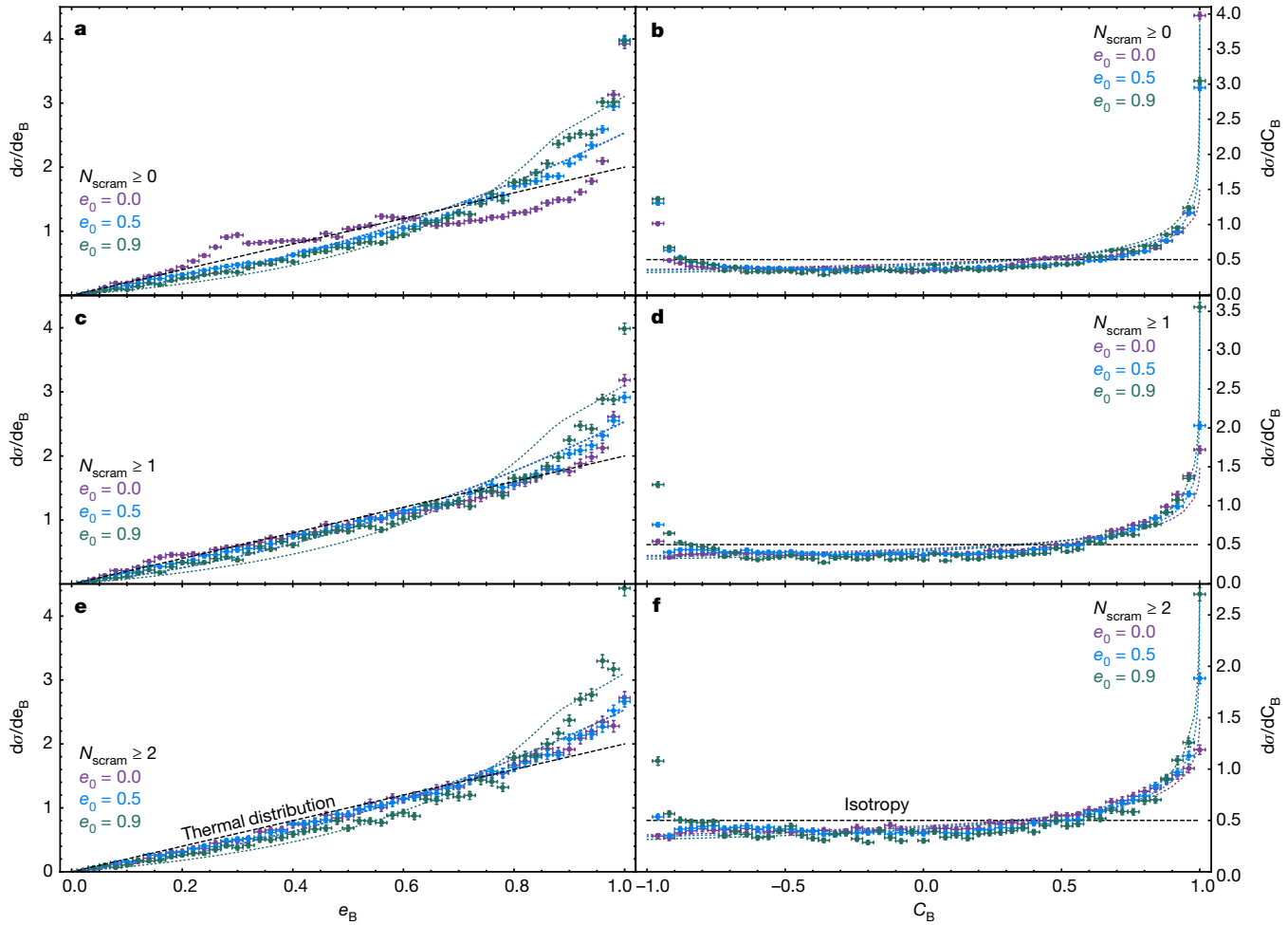

Fig. 4 | Marginal distributions of binary eccentricity and orientation. **a**, **c**, **e**, $d\sigma/de_B$ against eccentricity e_B. **b**, **d**, **f**, $d\sigma/dC_B$ against the cosine of the binary inclination, C_B. Line styles represent ergodic outcome distributions with the same ensemble angular momenta as in Fig. 3. The data points are binned outcomes from the same numerical scattering ensembles as in Fig. 3, with each row corresponding to the same cuts on N_{scram}. The eccentricity outcome distributions are notably super-thermal (the thermal distribution, $d\sigma/de_B = 2e$, is shown as a black dashed line). The inclination distributions exhibit anisotropic bias towards prograde binaries aligned with $\mathbf{L}_0$ (the isotropic distribution is shown with a black dashed line). Horizontal error bars show bin sizes and vertical error bars indicate 95% Poissonian confidence intervals.

has clear geometrical features indicative of prompt exchanges, these 'clouds of regularity' mostly (entirely) disappear if one considers the ~50% of integrations with $N_{scram} \geq 1$ ($N_{scram} \geq 2$). With this qualitative argument in mind, we use Figs. 3 and 4 to quantitatively compare the binned results of our scattering experiments to the marginal distributions predicted by the ergodic hypothesis. Horizontal error bars show bin sizes and vertical error bars indicate 95% Poissonian confidence intervals. All three of the marginal distributions that we examine ($d\sigma/dE_B$, $d\sigma/de_B$ and $d\sigma/dC_B$) exhibit reasonable (and sometimes very close) agreement between the ergodic theory of equation (2) and our numerical scattering experiments, provided that we examine resonant encounters ($N_{scram} \geq 2$). The marginal distributions for large-L_0 ensembles are very consistent with the numerical experiments. The agreement is slightly worse for our low-L_0 ensemble.

The agreement between ergodic theory and experiment is never exact, even in $N_{scram} \geq 2$ subsamples, and in most cases we see data that match analytic predictions to leading order but also exhibit some level of higher-order structure. The nature of these superimposed, second-order structures is not altogether clear, as two explanations seem plausible. First, these could represent islands of regularity in the initial conditions that we explore: regions of parameter space that do not fully forget their initial conditions despite undergoing multiple scrambles. Second, these could represent a failure in the idealized escape criteria, $R(E_B, L_B)$, that we employ. We only consider very simple definitions of the strong-interaction region, the true shape of which is probably connected to the stability boundary of the triple[24]. We defer an investigation of these two hypotheses to future work.

Non-hierarchical triples are common, if short-lived, in the astrophysical Universe[25]. They are responsible for many interesting phenomena. For example, binary–single scattering events in dense star clusters produce blue stragglers[26,27], cataclysmic variables[28], X-ray binaries[29,30] and even binary stellar-mass black holes[11]. The lattermost of these scenarios may be responsible for most of the black-hole mergers seen by the LIGO experiment[12,13]. Dynamical formation of these systems in a binary–single scattering is favoured when the surviving binary is drawn from the high-e_B tail of outcomes. It is therefore notable that (i) we find generic superthermality in the outcomes of comparable-mass scatterings (both from ergodic theory and numerical experiments) and (ii) that our formalism has identified the type of binary–single encounters that are predisposed to produce exotic binaries: low-L_0 scatterings. In the future, it may be possible to apply our formalism to estimate the properties of temporary binaries formed during long, but non-terminal, single-star ejections. High eccentricity binaries formed as 'intermediate states' of a three-body resonance may merge during the ejection owing to short-range dissipative

forces, leading to, for example, uniquely eccentric gravitational-wave signals[14].

Online content

Any methods, additional references, Nature Research reporting summaries, source data, extended data, supplementary information, acknowledgements, peer review information; details of author contributions and competing interests; and statements of data and code availability are available at https://doi.org/10.1038/s41586-019-1833-8.

1. Agekyan, T. A. & Anosova, Z. P. A study of the dynamics of triple systems by means of statistical sampling. *Astron. Zh.* **44**, 1261 (1967).
2. Šuvakov, M. & Dmitrašinović, V. Three classes of Newtonian three-body planar periodic orbits. *Phys. Rev. Lett.* **110**, 114301 (2013).
3. Standish, E. M. The dynamical evolution of triple star systems. *Astron. Astrophys.* **21**, 185–191 (1972).
4. Hut, P. & Bahcall, J. N. Binary–single star scattering. I – numerical experiments for equal masses. *Astrophys. J.* **268**, 319–341 (1983).
5. Poincaré, H. *Les Méthodes Nouvelles de la Mécanique Céleste* (Gauthier-Villars et fils, 1892).
6. Sundman, K. F. Mémoire sur le problème des trois corps. *Acta Math.* **36**, 105–179 (1913).
7. Fermi, E. High energy nuclear events. *Prog. Theor. Phys.* **5**, 570–583 (1950).
8. Monaghan, J. J. A statistical theory of the disruption of three-body systems – I. Low angular momentum. *Mon. Not. R. Astron. Soc.* **176**, 63–72 (1976).
9. Valtonen, M., Mylläri, A., Orlov, V. & Rubinov, A. Dynamics of rotating triple systems: statistical escape theory versus numerical simulations. *Mon. Not. R. Astron. Soc.* **364**, 91–98 (2005).
10. Heggie, D. C. Binary evolution in stellar dynamics. *Mon. Not. R. Astron. Soc.* **173**, 729–787 (1975).
11. Portegies Zwart, S. F. & McMillan, S. L. W. Black hole mergers in the Universe. *Astrophys. J. Lett.* **528**, 17–20 (2000).
12. Rodriguez, C. L., Chatterjee, S. & Rasio, F. A. Binary black hole mergers from globular clusters: masses, merger rates, and the impact of stellar evolution. *Phys. Rev. D* **93**, 084029 (2016).
13. Hong, J. et al. Binary black hole mergers from globular clusters: the impact of globular cluster properties. *Mon. Not. R. Astron. Soc.* **480**, 5645–5656 (2018).
14. Samsing, J., MacLeod, M. & Ramirez-Ruiz, E. The formation of eccentric compact binary inspirals and the role of gravitational wave emission in binary–single stellar encounters. *Astrophys. J.* **784**, 71 (2014).
15. Rodriguez, C. L. et al. Post-Newtonian dynamics in dense star clusters: formation, masses, and merger rates of highly-eccentric black hole binaries. *Phys. Rev. D* **98**, 123005 (2018).
16. Portegies Zwart, S. F. & Boekholt, T. C. N. Numerical verification of the microscopic time reversibility of Newton's equations of motion: fighting exponential divergence. *Commun. Nonlinear Sci. Numer. Simul.* **61**, 160–166 (2018).
17. Hut, P. The topology of three-body scattering. *Astron. J.* **88**, 1549–1559 (1983).
18. Samsing, J. & Ilan, T. Topology of black hole binary–single interactions. *Mon. Not. R. Astron. Soc.* **476**, 1548–1560 (2018).
19. Bohr, N. Neutron capture and nuclear constitution. *Nature* **137**, 344–348 (1936).
20. Monaghan, J. J. A statistical theory of the disruption of three-body systems – II. High angular momentum. *Mon. Not. R. Astron. Soc.* **177**, 583–594 (1976).
21. Nash, P. E. & Monaghan, J. J. A statistical theory of the disruption of three-body systems – III. Three-dimensional motion. *Mon. Not. R. Astron. Soc.* **184**, 119–125 (1978).
22. Geller, A. M., Leigh, N. W. C., Giersz, M., Kremer, K. & Rasio, F. A. In search of the thermal eccentricity distribution. *Astrophys. J.* **872**, 165 (2019).
23. Pomeau, Y. & Manneville, P. Intermittent transition to turbulence in dissipative dynamical systems. *Commun. Math. Phys.* **74**, 189–197 (1980).
24. Mardling, R. A. & Aarseth, S. J. Tidal interactions in star cluster simulations. *Mon. Not. R. Astron. Soc.* **321**, 398–420 (2001).
25. Leigh, N. W. C. & Geller, A. M. The dynamical significance of triple star systems in star clusters. *Mon. Not. R. Astron. Soc.* **432**, 2474–2479 (2013).
26. Leonard, P. J. T. & Fahlman, G. G. On the origin of the blue stragglers in the globular cluster NGC 5053. *Astron. J.* **102**, 994 (1991).
27. Leigh, N., Sills, A. & Knigge, C. An analytic model for blue straggler formation in globular clusters. *Mon. Not. R. Astron. Soc.* **416**, 1410–1418 (2011).
28. Ivanova, N. et al. Formation and evolution of compact binaries in globular clusters – I. Binaries with white dwarfs. *Mon. Not. R. Astron. Soc.* **372**, 1043–1059 (2006).
29. Pooley, D. & Hut, P. Dynamical formation of close binaries in globular clusters: cataclysmic variables. *Astrophys. J. Lett.* **646**, 143–146 (2006).
30. Ivanova, N., Heinke, C. O., Rasio, F. A., Belczynski, K. & Fregeau, J. M. Formation and evolution of compact binaries in globular clusters – II. Binaries with neutron stars. *Mon. Not. R. Astron. Soc.* **386**, 553–576 (2008).

Data availability

The data that support the findings of this study are available from the corresponding author upon reasonable request.

Acknowledgements We acknowledge discussions with D. Heggie, P. Hut, R. Sari and S. Portegies-Zwart, as well as feedback from E. Michaely and O. C. Winter. N.C.S. received financial support from NASA, through Einstein Postdoctoral Fellowship Award number PF5-160145 and the NASA Astrophysics Theory Research Program (grant NNX17AK43G; Principal Investigator, B. Metzger). N.C.S. also thanks the Aspen Center for Physics for its hospitality during early stages of this work. N.W.C.L. acknowledges support by Fondecyt Iniciacion grant number 11180005. We thank the Chinese Academy of Sciences for hosting us as we completed our efforts. We thank M. Valtonen and H. Karttunen, whose book on the three-body problem motivated much of this work.

Author contributions N.C.S. led the analytic work, to which N.W.C.L. contributed significantly. The FEWBODY simulations were performed by N.W.C.L. The comparison between the simulations and the analytic theory was performed jointly by the two authors.

Competing interests The authors declare no competing interests.

Additional information
Supplementary information is available for this paper at https://doi.org/10.1038/s41586-019-1833-8.
Correspondence and requests for materials should be addressed to N.C.S.
Peer review information *Nature* thanks Erez Michaely and Othon Cabo Winter for their contribution to the peer review of this work.
Reprints and permissions information is available at http://www.nature.com/reprints.

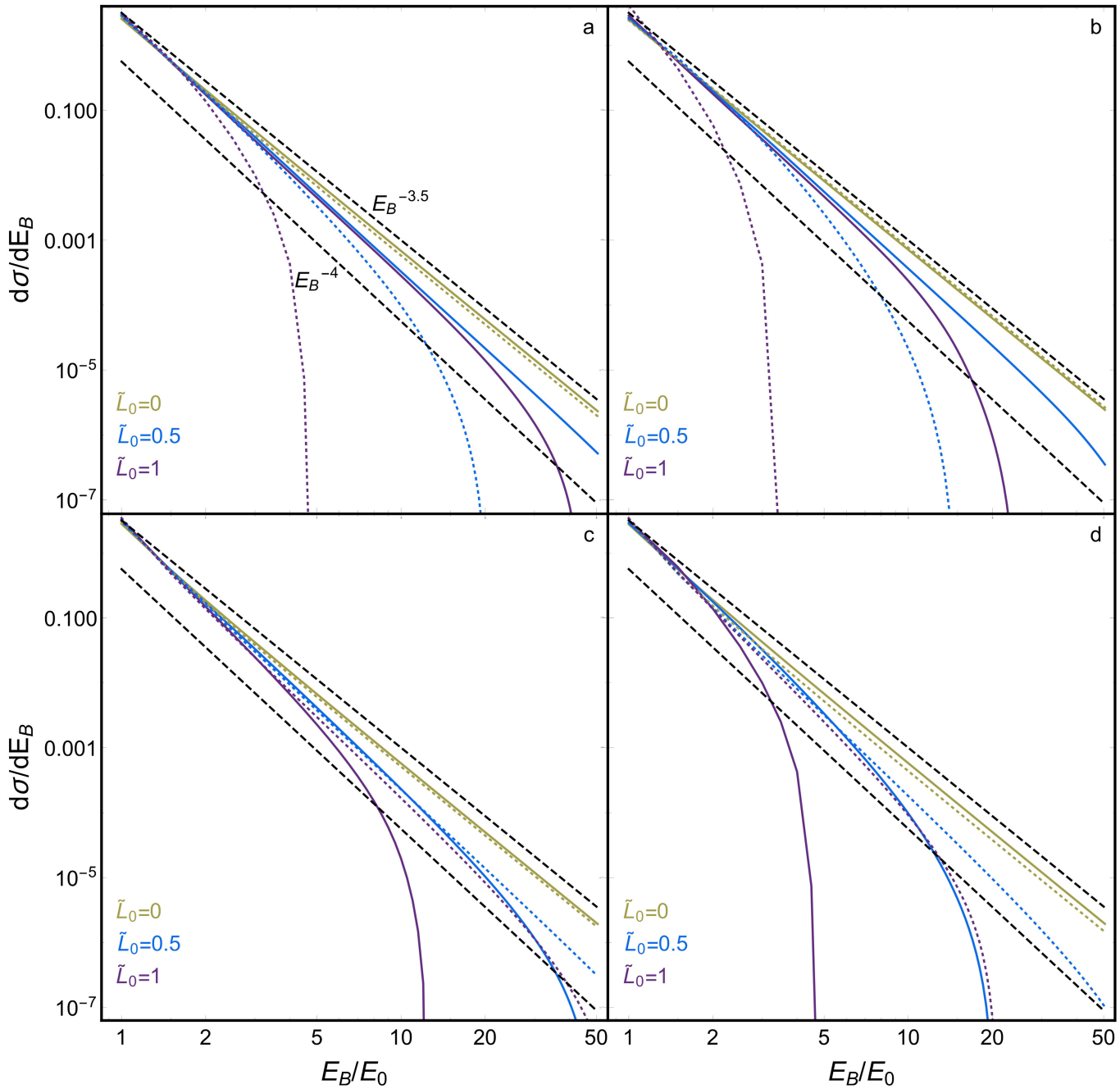

Extended Data Fig. 1 | Marginal distribution of binary energies, $d\sigma/dE_B$. Colours show dimensionless angular momenta $\tilde{L}_0$; upper and lower black dashed lines are asymptotic power laws for $\tilde{L}_0 = 1$ and $\tilde{L}_0 \approx 1$, respectively. **a**, Ergodic outcome distributions using the 'apocentric escape' (AE) criterion; that is, assuming that disintegration of metastable triples occurs within a strong interaction region of size $R = \alpha a_B(1 + e_B)$. Here we take $\alpha = 2$. Solid lines represent equal-mass scattering ensembles ($m_a = m_b = m_s$) and dotted lines extreme-mass-ratio ensembles ($m_a = m_b = 10m_s$). **b**, As in **a**, but for a 'simple escape' (SE) criterion, $R = \alpha a_B$. **c**, Intermediate-mass-ratio scattering ensembles ($m_a = m_b = 3m_s$). Solid lines correspond to $\alpha = 2$ and dotted lines to $\alpha = 5$. **d**, As in **c**, but for $m_a = m_b = 10m_s$. Note that $\tilde{L}_0$ is a dimensionless angular momentum normalized by the circular orbit angular momentum of a binary with energy E_0 and masses m_a and m_b.

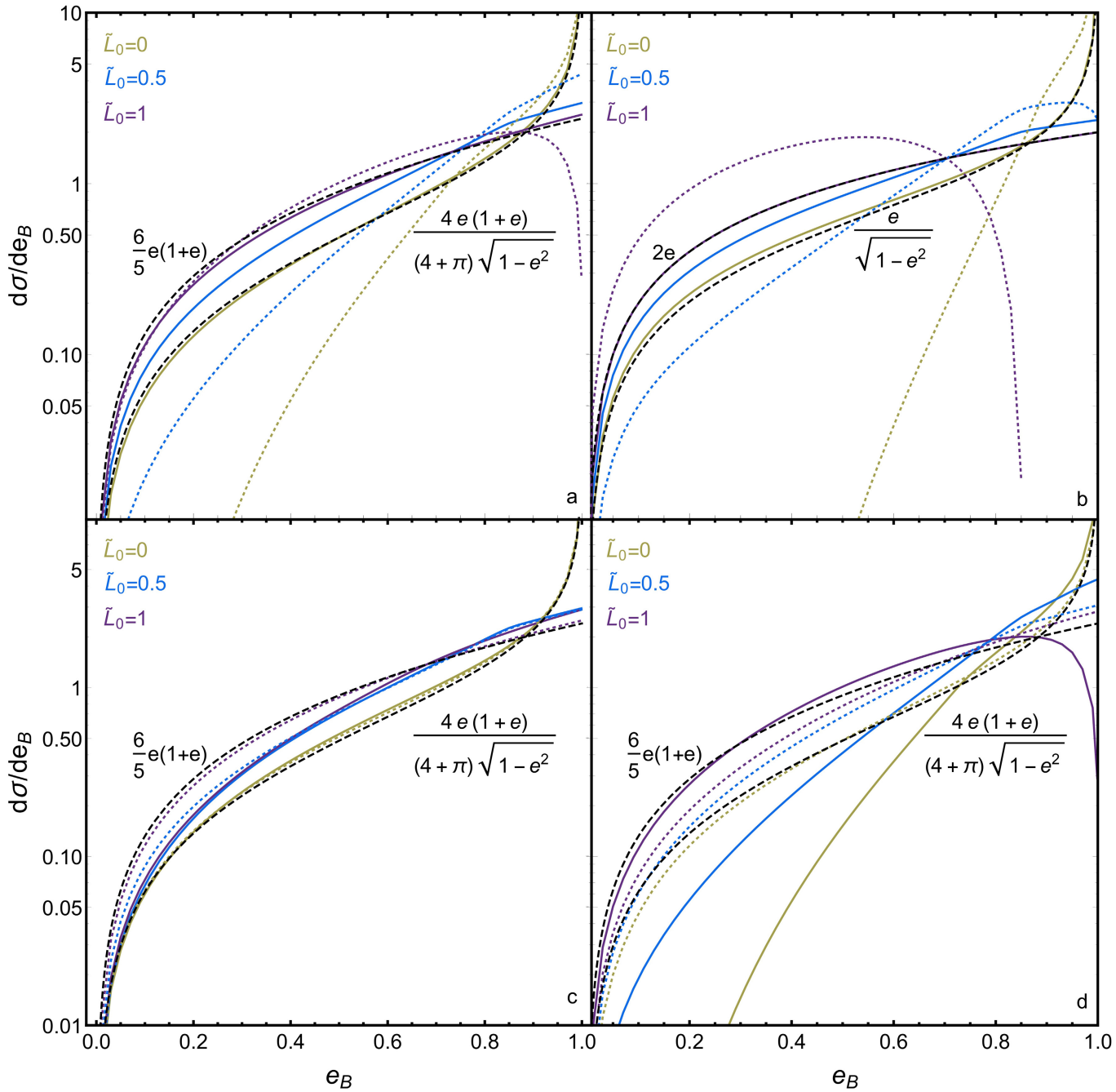

Extended Data Fig. 2 | Marginal distribution of binary eccentricity, dσ/de$_B$. Line styles and assumptions are as in Extended Data Fig. 1, except for the upper and lower black dashed lines, which here show the $\tilde{L}_0 \approx 1$ and $\tilde{L}_0 \ll 1$ limits of the dσ/de$_B$ distribution, respectively (unlike for dσ/dE_B, these limits differ significantly in the AE and SE regimes). In comparable-mass AE calculations, mildly super-thermal outcomes arise from geometric effects when $\tilde{L}_0 \approx 1$; by contrast, angular-momentum starvation produces extremely super-thermal outcomes when $\tilde{L}_0 \ll 1$. Small m_s values foreclose parts of e_B space, as $L_B \approx L_0$.

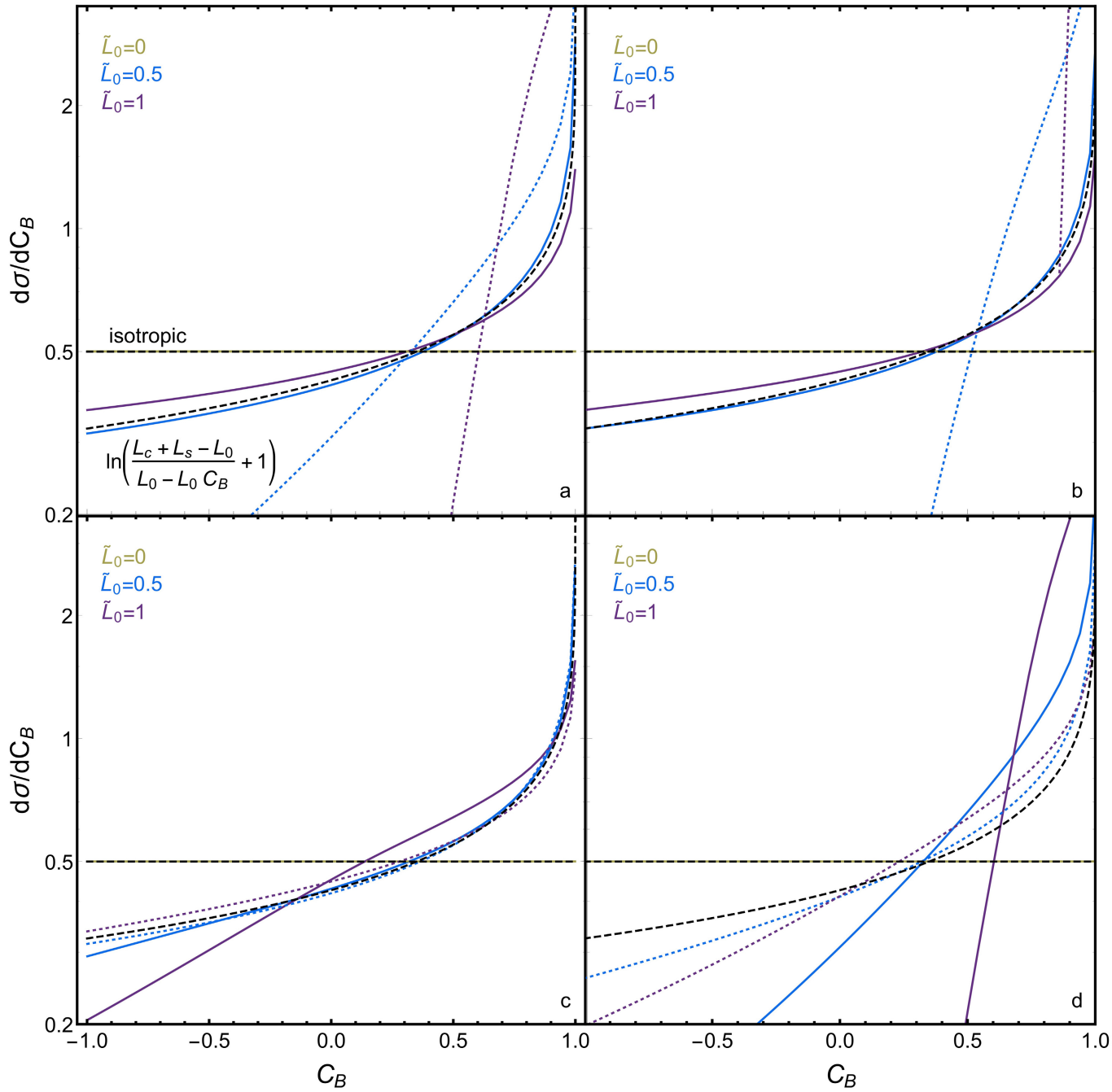

Extended Data Fig. 3 | Marginal distribution of binary orientation, $d\sigma/dC_B$. Assumptions and line styles are as in Extended Data Fig. 1, except that the black dashed lines show (i) an isotropic outcome configuration and (ii) an analytic approximation for $d\sigma/dC_B$, as labelled in **a** (for an equal-mass triple with $\tilde{L}_0 = 0.5$). For $\tilde{L}_0 \ll 1$, surviving binaries are distributed isotropically (as symmetry dictates). Otherwise, binary orientations $C_B = \hat{\mathbf{L}}_B \cdot \hat{\mathbf{L}}_0$ are biased towards prograde outcomes. For extreme mass ratios and large $\tilde{L}_0$, retrograde outcomes may be entirely prohibited.

Extended Data Table 1 | Numerical (binary–single) scattering ensembles used for comparison to analytic theory

Run	e_0	$\tilde{L}_0$	N_0	N_1	N_2
A	0.0	1.0	116,993	56,696	39,819
B	0.5	0.87	121,328	65,936	51,791
C	0.9	0.44	107,992	76,051	46,852

The first two columns show the initial binary eccentricity e_0 and the conserved dimensionless angular momentum $\tilde{L}_0$ in each simulated scattering run. The other columns show the number of runs with $N_{scram} \geq I$, N_I. Each run has initial impact parameter $b = 0$, isotropically distributed phase angles and particles of equal mass ($m_a = m_b = m_s$).